PENNSTATE

AEROSPACE 305W STRUCTURES & DYNAMICS LABORATORY

Laboratory Experiment #3

Beam Vibration

April 21, 2011

Brett Davis

Lab Section #17

Lab Partners:

Titos Gosalves

Kevin Harrigan

James Trexler

Zachary Watson

Course Instructor: Dr. Stephen Conlon

Lab TA: *Kevin Brennan*

Abstract

The objective of this experiment was to investigate beam vibrations. Specifically: mode shape, natural frequency and damping ratio were examined. Additionally, four different sensors were used to collect data in order to determine their usefulness in such applications. The four sensors were and accelerometer, Laser Doppler Vibrometer (LDV), piezoelectric strain sensor and a strain gauge. Aerospace structures are often subjected to dynamic forces and vibrations. It is important to understand the effects of such forces on a structure, as well as the significance of resonance. Resonance frequencies are always a major design consideration in any field and especially in aerospace engineering. In this experiment an electromechanical vibration exciter was used to vibrate a long slender beam. The shaker was not designed to operate at some of the lower frequencies used in the experiment, and may have contributed to the error at these low frequencies. Other sources of error included signal noise, the accelerometer being mounted with wax, torsional vibration modes of the beam and resonance frequencies of the experimental apparatus such as the work bench. The natural frequencies were measured by adjusting the input frequency until the largest signal oscillations were seen on an oscilloscope. These frequencies were close to the theoretical values with less than 18% error; most of the error could be due to the model not accounting for damping in the system. The damping ratios decreased as the natural frequencies increased as expected. The locations of the nodes closely matched the predicted values. The frequencies for each vibration mode decreased slightly when the accelerometer was mounted, as it added mass to the tip of the beam. This was consistent with what was expected and shows the drawback of mounting a heavier sensor on the specimen as it alters the frequencies of vibration. The natural frequencies were also determined using spectrum analysis. The natural frequencies determined using this method were comparable to those found with the oscilloscope, but were obtained much faster. All four sensors showed high coherence at the natural frequencies. The piezoelectric sensor gave the best results for phase shifts, which allowed the resonance frequencies to be confirmed to be those of the beam and not of the experimental setup or from a torsional mode.

Results and Discussion

Figure 1 shows the theoretical mode shapes of the beam with no tip mass and the measured node points. The measured locations of the nodes closely matched the theoretical mode shapes at every location. The small deviations can be attributed to the error in measure their locations by hand with a tape measure.

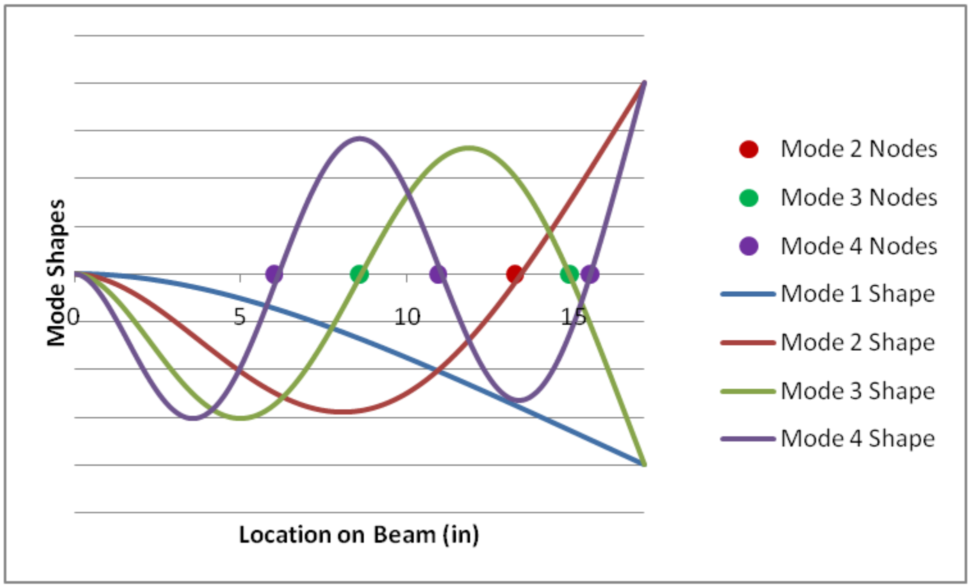

Figure 1. Mode Shapes and Node Locations without Tip Mass

Table 1 shows the measured locations of the nodes for both with and without the tip mass. The addition of the tip mass caused the nodes to move slightly further down the beam as expected. The only node that did not move further down the beam was the 2nd node in mode 4. This node remained 6 inches from the clamped end of the beam in both configurations.

Table 1. Measured Node Locations

Mode and Configuration	1st Node	2nd Node	3rd Node	4th Node
Mode 1 (No Mass)	**0”**	**-**	**-**	**-**
Mode 2 (No Mass)	**0”**	**13 1/4”**	**-**	**-**
Mode 3 (No Mass)	**0”**	**8 9/16”**	**14 7/8”**	**-**
Mode 4 (No Mass)	**0”**	**6”**	**10 15/16”**	**15 1/2”**
Mode 1 (Tip Mass)	**0”**	**-**	**-**	**-**
Mode 2 (Tip Mass)	**0”**	**13 5/8”**	**-**	**-**
Mode 3 (Tip Mass)	**0”**	**8 7/8”**	**15 3/16”**	**-**
Mode 4 (Tip Mass)	**0”**	**6”**	**11 1/4”**	**15 3/4”**

The natural frequencies obtained by adjusting the input frequency until the maximum tip deflections were found were close to the predicted theoretical frequencies. Figure 2 and Table 2 show that the natural frequencies were close to the theoretical values predicted. The highest error was 17.5% for the natural frequency in mode 2 without the tip mass. The main source of error was that the theoretical model does not account for any damping in the system. Mode 1's natural frequency decreased with the addition of the tip mass from 13 Hz to 12 Hz. The other three modes decreased as well when the tip mass was added. This change in frequency is consistent with the theoretical values as can be seen in Table 2.

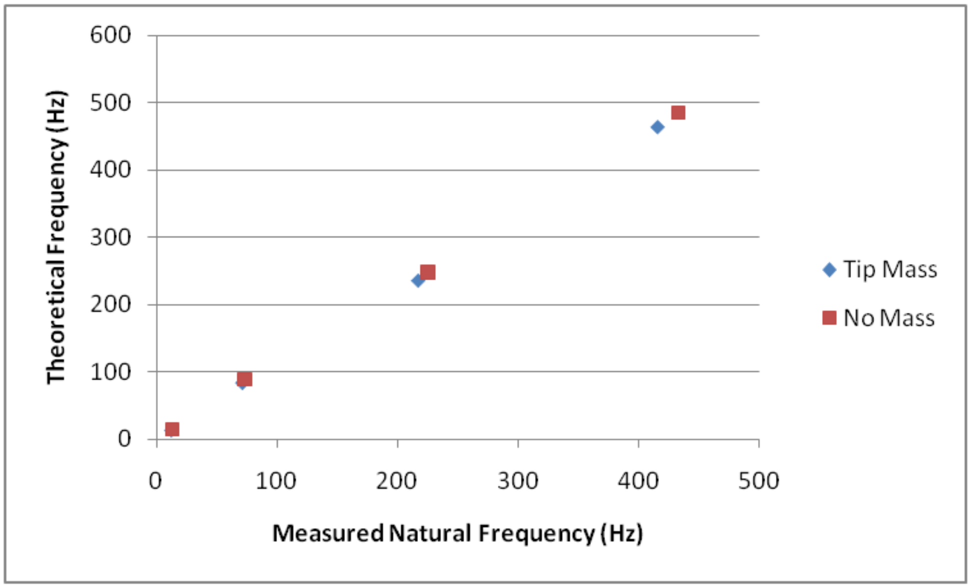

Figure 2. Measured and Theoretical Natural Frequency

Table 2. Measured and Theoretical Natural Frequencies

Mode	Measured Frequency Hz	Theoretical Frequency Hz	% Error
Mode 1 (No Mass)	**13**	**14.12**	**-7.93**
Mode 2 (No Mass)	**73**	**88.49**	**-17.50**
Mode 3 (No Mass)	**225**	**247.82**	**-9.21**
Mode 4 (No Mass)	**433**	**485.20**	**-10.76**
Mode 1 (Tip Mass)	**12**	**13.32**	**-9.88**
Mode 2 (Tip Mass)	**71**	**83.91**	**-15.38**
Mode 3 (Tip Mass)	**217**	**235.95**	**-8.03**
Mode 4 (Tip Mass)	**416**	**464.15**	**-10.37**

The damping ratios of the beam are shown for each natural frequency measured during the experiment in Figure 3. The Figure shows that the damping ratios decreased as the natural frequency increased. It can also be seen that the damping ratios for the tip mass configuration were higher than the damping ratios for the beam without the tip mass. This is consistent with the decreased frequencies for the tip mass beam. The higher damping values decrease the observed frequency of oscillation. Table 3 gives the values for the damping ratios at each frequency.

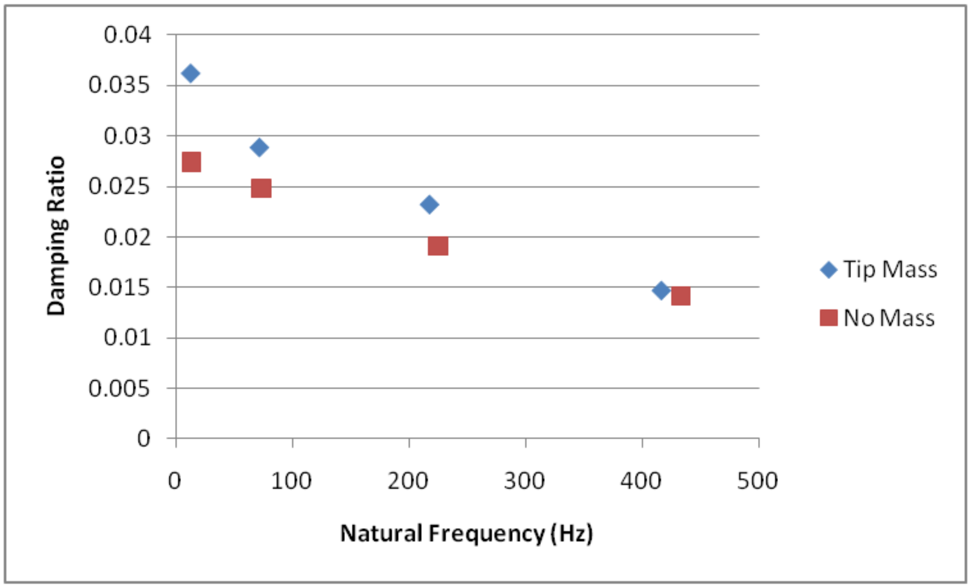

Figure 3. Damping Ratio and Natural Frequency

Table 3. Damping Ratios and Natural Frequency

Mode	Frequency (Hz)	Damping Ratio
Mode 1 (No Mass)	**13**	**0.0274**
Mode 2 (No Mass)	**73**	**0.0248**
Mode 3 (No Mass)	**225**	**0.0191**
Mode 4 (No Mass)	**433**	**0.0141**
Mode 1 (Tip Mass)	**12**	**0.0362**
Mode 2 (Tip Mass)	**71**	**0.0289**
Mode 3 (Tip Mass)	**217**	**0.0232**
Mode 4 (Tip Mass)	**416**	**0.0147**

The other method used to determine the resonance frequencies was by using a spectrum analyzer. Figure 4 through 7 show the magnitude of the frequency responses. Each peak indicates a possible resonance frequency of the beam. Data was taken with an accelerometer (the tip mass), Laser Doppler Vibrometer (LDV), piezoelectric strain sensor and strain gauge.

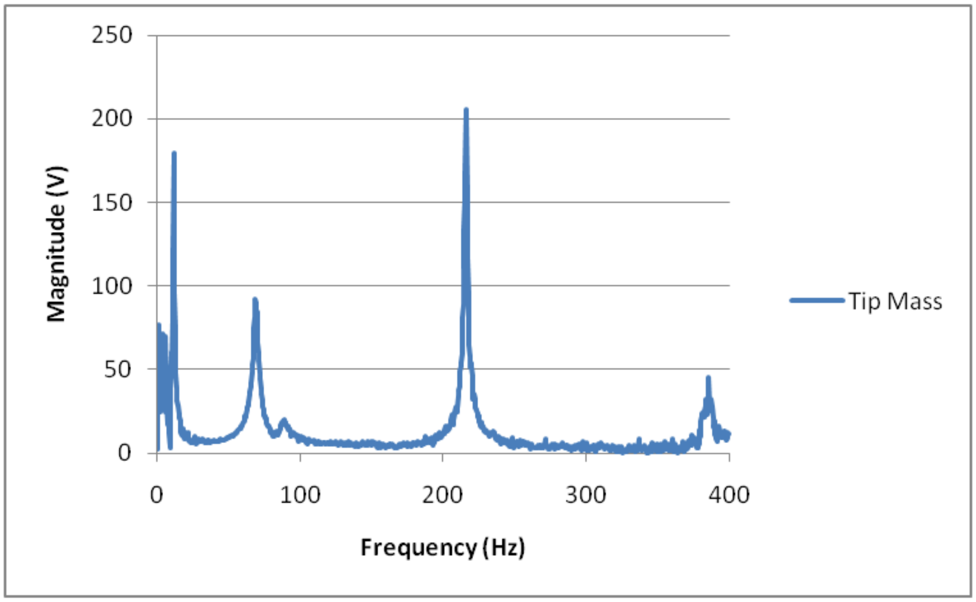

Figure 4. Accelerometer, Frequency Response Magnitude

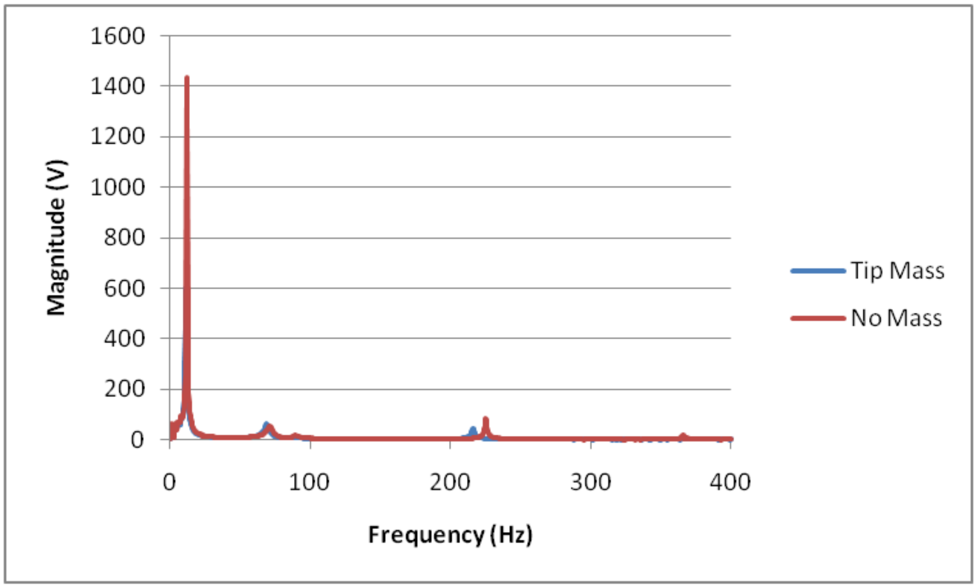

Figure 5. LDV, Frequency Response Magnitude

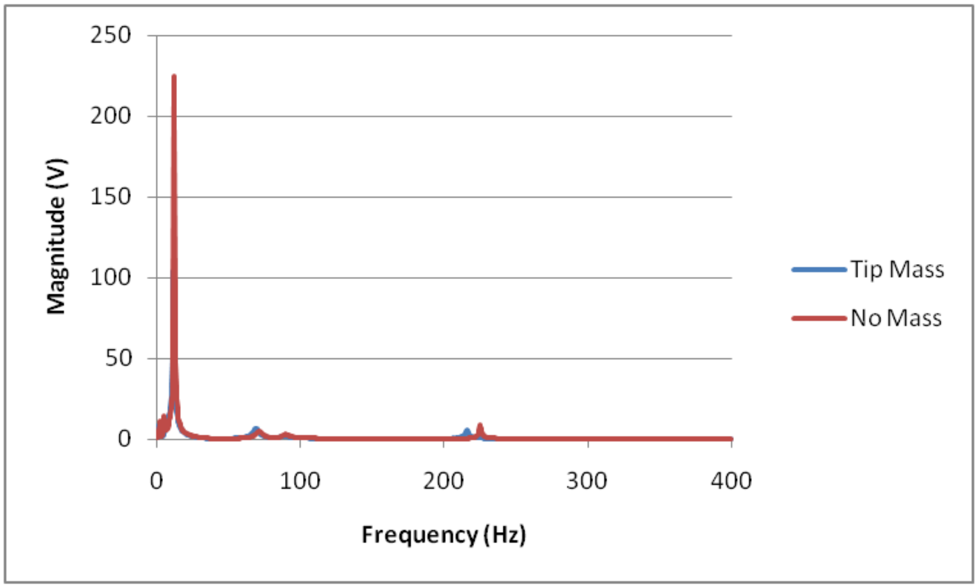

Figure 6. Piezoelectric Strain Sensor, Frequency Response Magnitude

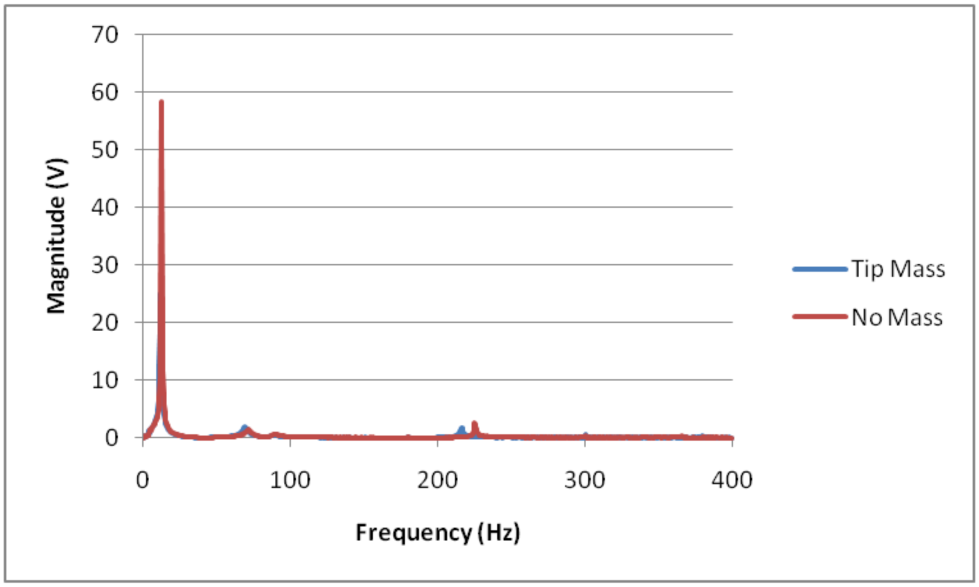

Figure 7. Strain Gauge, Frequency Response Magnitude

The LDV, strain sensor and strain gauge all had high magnitudes at 12.11 Hz for both with and without the tip mass. Their other peaks were considerably lower, but still distinguishable. At the higher frequencies, the tip mass beam had slightly lower frequencies; however, at low frequencies the peaks coincided. In Figure 4, it can be seen that the accelerometer produced higher peaks at high frequencies compared to the other three sensors, which made determining the resonance frequencies easier. From Figure 4, it can also be seen that there was an additional peak at 83 Hz. A very small peak can be seen on Figures 5 through 7 at 85 Hz. This frequency was not seen in the previous method of locating resonance frequencies. This frequency could be due to a resonance frequency of the table or other apparatus near the experiment. The LDV without a tip mass had an additional peak at 363 Hz and the accelerometer had one at 385.5 Hz. These could possibly be the 4th mode's resonance frequency, but t should be noted that the frequency response data was for 0 to 400 Hz, therefore the resonance frequency of the 4th modes were not able to be reliably determined using this method. Future experiments should include a range of frequencies that captures all resonance frequencies of interest. Table 4 gives the peak frequencies for each sensor and the resonance frequencies from Table 2.

Table 4. Natural Frequencies

Mode	Frequency (Hz)					
Methods	**Accelerometer**	**LDV**	**Pizo Strain Sensor**	**Strain Gauge**	**Previously Measured**	**Theoretical**
Mode 1 (No Mass)	**-**	**12.11**	**12.11**	**12.11**	**13**	**14.12**
Mode 2 (No Mass)	**-**	**69.9**	**68.34**	**67.97**	**73**	**88.49**
Mode 3 (No Mass)	**-**	**225.8**	**225**	**224.22**	**225**	**247.82**
Mode 4 (No Mass)	**-**	**-**	**-**	**-**	**433**	**485.20**
Mode 1 (Tip Mass)	**11.72**	**12.11**	**12.11**	**12.11**	**12**	**13.32**
Mode 2 (Tip Mass)	**68.75**	**70.7**	**70.7**	**68.35**	**71**	**83.91**
Mode 3 (Tip Mass)	**216.02**	**214.8**	**214**	**214.06**	**217**	**235.95**
Mode 4 (Tip Mass)	**-**	**-**	**-**	**-**	**416**	**464.15**

Figures 8 through 11 show the coherence for the signals from the four sensors. Figure 8 shows that the accelerometer had a coherence of 0.7 at the first resonance frequency around 12 Hz. The coherence was over 0.9 in the range of the second natural frequency at approximately 70 Hz. There was a large spike in the coherence at 216 Hz which was the 3rd natural frequency. The coherence was rising to 0.7 at 400 Hz, which was the end of the data collected and close to the 4th resonance frequency. The LDV also showed high coherence at the natural frequencies as seen in Figure 9. The LDV coherence was above 0.9

for the first two frequencies, and it was above 0.8 for the third frequency. There was a coherence of 0.5 near 363 Hz which corresponds to the peak magnitude seen in Figure 5.

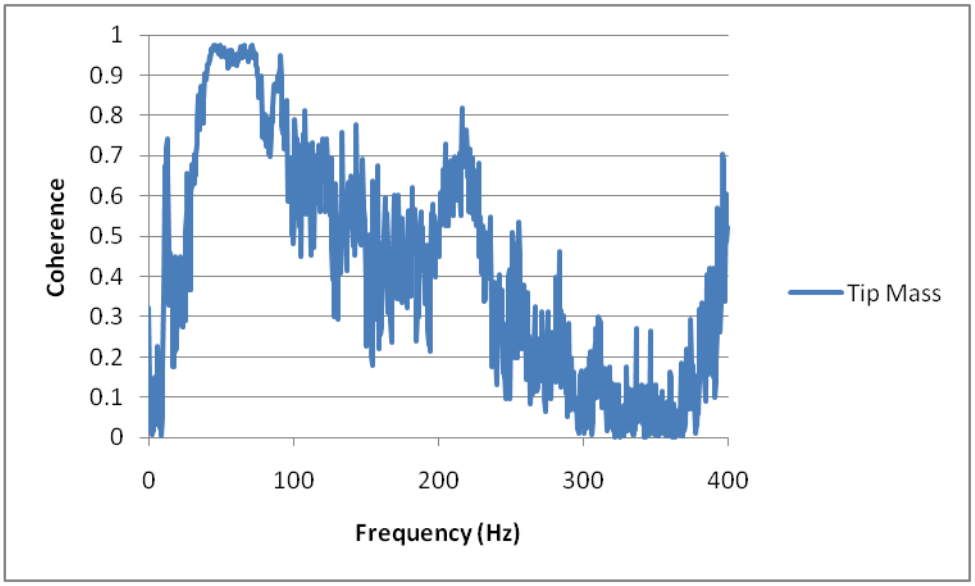

Figure 8. Accelerometer, Coherence

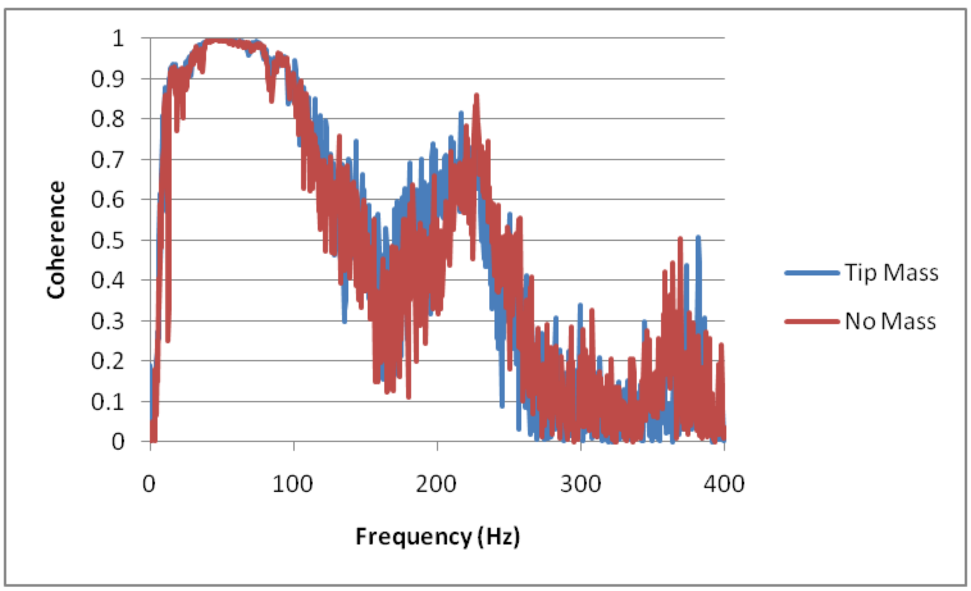

Figure 9. LDV, Coherence

Figure 10 shows the coherence for the piezoelectric strain sensor. As in Figures 8 and 9, there was coherence over 0.9 for frequencies from around 0 to 100 Hz. The second rise in coherence, to 0.8, occurred near the 3rd mode resonance frequencies at about 220Hz. Figure 4 shows the coherence of the strain gauge's signal. It is consistent with the strain sensor's coherence, except the strain gauge has a more dramatic rise in coherence at the resonance frequencies. Figures 8 through 11 show that all four of the sensors had high coherence at the resonance frequencies indicating they were reliable methods for determining the resonance frequencies as they all had a strong correlation between the input frequency and the measured response at the resonance frequencies. The accelerometer, LDV and strain gauge had the most dramatic rise in coherence at the resonance frequencies. The data with and without the tip mass were comparable in all cases, with only a small shift in frequency as expected.

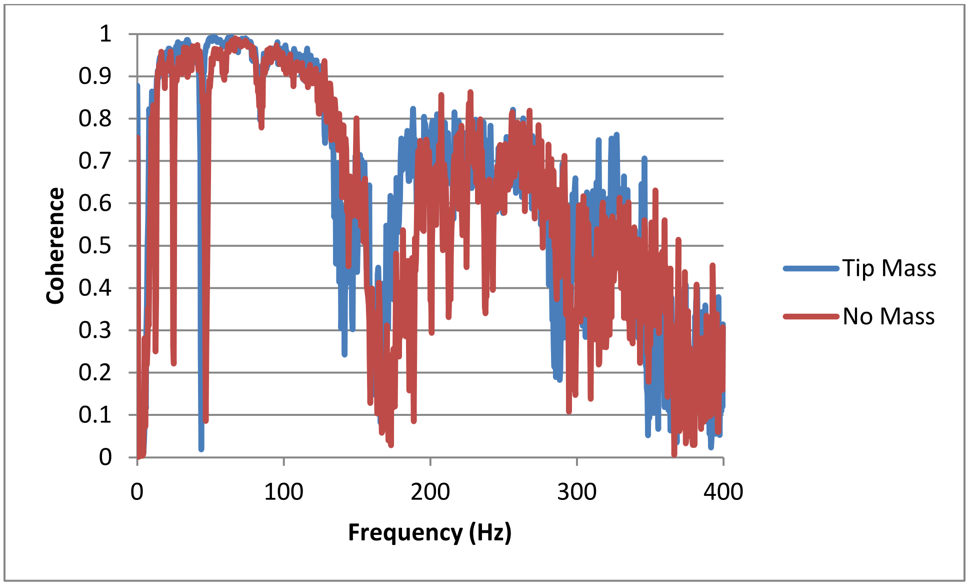

Figure 10. Piezoelectric Strain Sensor, Coherence

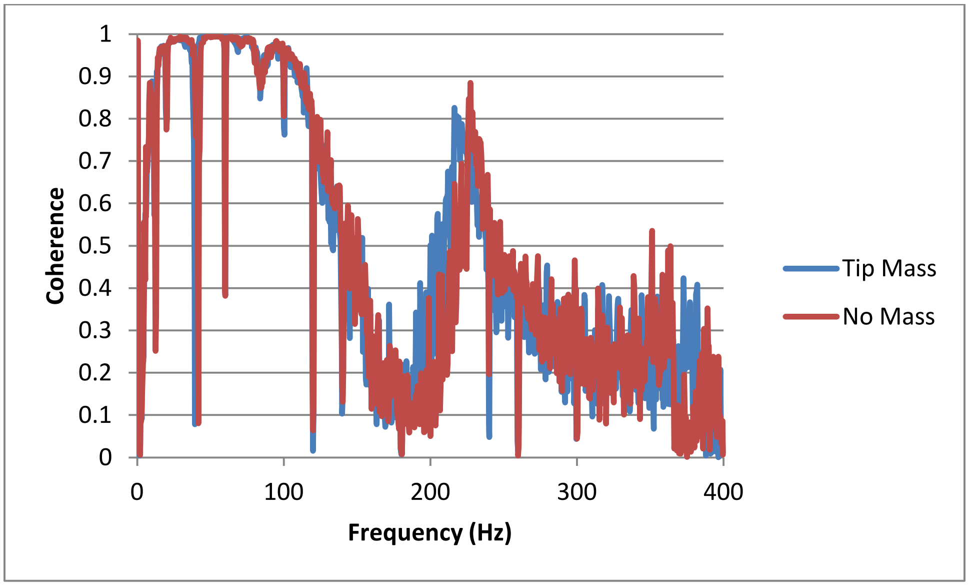

Figure 11. Strain Gauge, Coherence

Figures 12 through 15 show the phase of the fours sensors. The Accelerometer and LDV phase diagrams in Figures 12 and 13 show clear 180 degree phase shifts around 12 Hz and 216 Hz in the tip mass case and 12 and 225 Hz without a tip mass for the LDV. The expected phase shift at the second resonance frequency around 70 Hz is hard to distinguish from the other frequency peak seen at 85 Hz in Figures 12 and 13. Figure 14, the piezoelectric strain sensor, shows the best results for the phase shifts. There are 180 degree shifts at 12 Hz, 70 Hz and 216 Hz for the beam with the tip mass and 12 Hz, 73 Hz and 225 Hz without the mass. From the strain sensor data in Figure 14, it can be seen that the phase shift at 85 Hz is not 180 degree so it is likely not a resonance frequency of the beam, but rather that of the table or another part of the experimental apparatus. The Accelerometer, LDV and strain gauge data show this also, but it is easiest to decipher in Figure 14 with the piezoelectric stain sensor. The strain gauge's data for the phase shifts is fairly unclear throughout, while the strain sensor's data is by far the clearest. From Figures 12 through 15 it appears there is a 180 degree shift between 360 to 390 Hz, where peaks in magnitude were seen in Figures 4 and 5. This could be the fourth resonance frequencies of the beams; however the data ends at 400 Hz so it is difficult to tell exactly what is happening. A larger range of frequencies should be examined to determine the fourth mode frequencies and the causes of these two peaks.

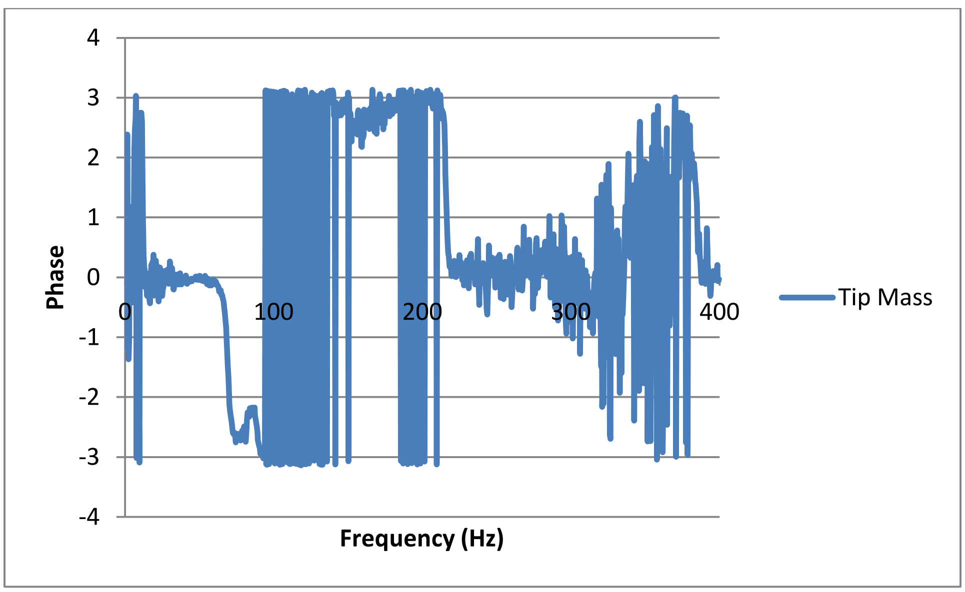

Figure 12. Accelerometer, Phase

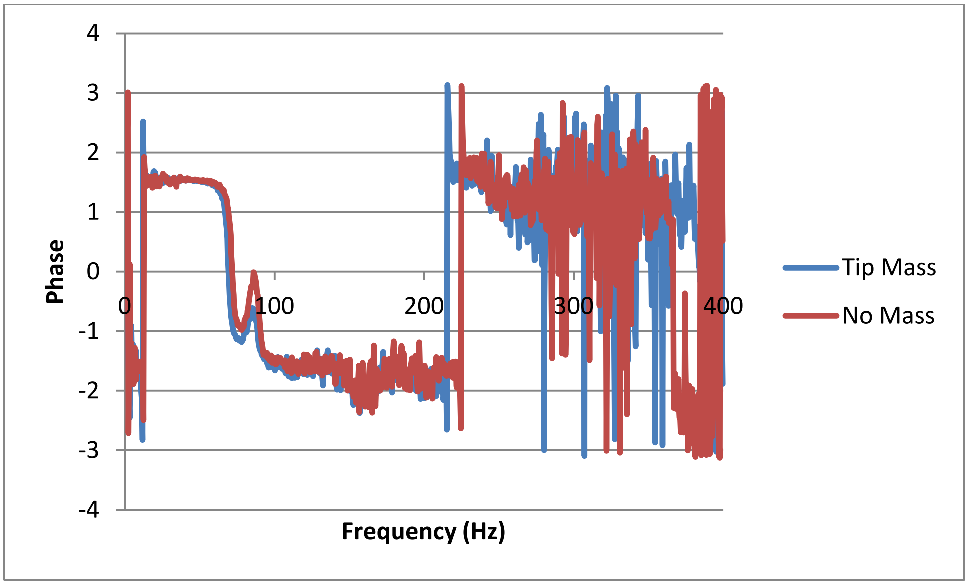

Figure 13. LDV, Phase

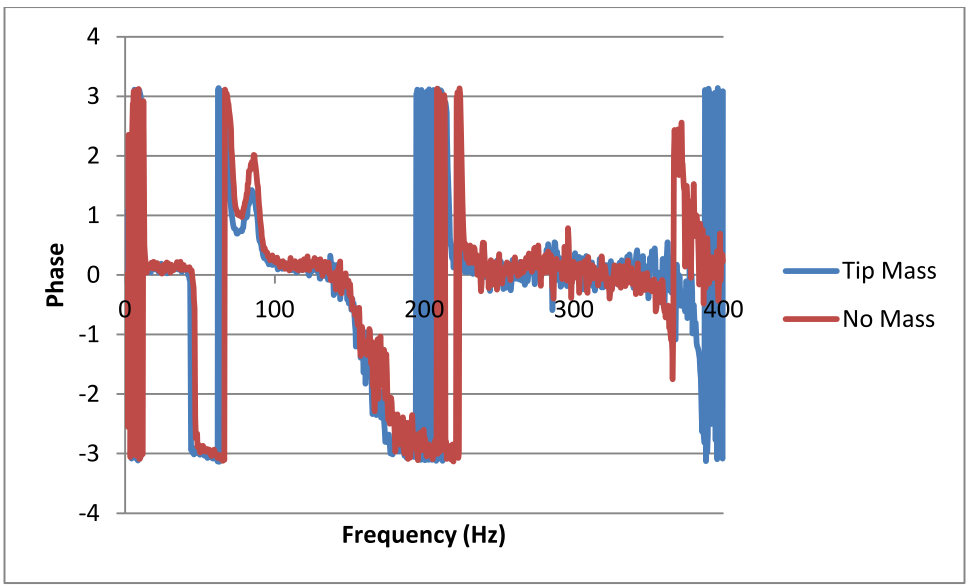

Figure 14. Piezoelectric Strain Sensor, Phase

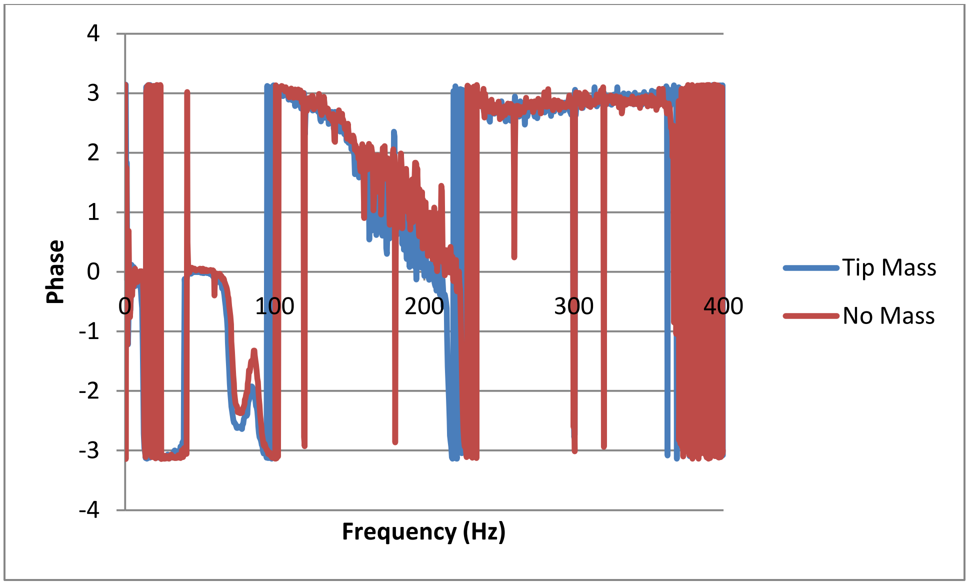

Figure 15. Strain Gauge, Phase

This experiment showed that an accelerometer, LDV, piezoelectric strain sensor and strain gauge can all be used to determine the natural frequencies of vibration of a beam. The accelerometer gave the best results for the magnitude plot, as it had easily identifiable peaks. The piezoelectric sensor's phase diagram was the clearest, while the strain gauge's was too fluctuating to be of much use. The accelerometer's coherence was the best, while the piezoelectric sensor's was worst but still useful.